# Long-term trends (1958–2017) in snow cover duration and depth in the Pyrenees

Juan Ignacio López Moreno, Jean-Michel Soubeyroux, Simon Gascoin, E. Alonso-gonzalez, Nuria Durán-gómez, Matthieu Lafaysse, Matthieu Vernay, Carlo Maria Carmagnola, Samuel Morin

# LONG TERM TRENDS (1958–2017) IN SNOW COVER DURATION AND DEPTH IN THE PYRENEES

**Running tittle: Trends in snow cover in the Pyrenees**

**López-Moreno, J.I[1]; Soubeyroux J.M. [2]; Gascoin, S.[3]; Alonso-Gonzalez[1]; Durán-Gómez, N.[2], Lafaysse, M. [4], Vernay, M. [4], Carmagnola, C.[4]; Morin, S. [4]**

1. Pyrenean Institute of Ecology, CSIC. Avda Montañana 1005. Zaragoza, Spain

2. Meteo France, Toulouse, France

3. Centre d'Etudes Spatiales de la Biosphère (CESBIO), Université de Toulouse, CNRS/CNES/IRD/INRA/UPS, 31400 Toulouse, France

4. Univ. Grenoble Alpes, Université de Toulouse, Météo-France, Grenoble, France, CNRS, CNRM, Centre d'Etudes de la Neige, 38000 Grenoble, France.

Corresponding author:

Juan Ignacio López Moreno

Pyrenean Institute of Ecology. CSIC

Avda Montañana 1005. Zaragoza 50.059. Spain

Tel : 0034976369393

Email : nlopez@ipe.csic.es

**Abstract.** This study investigated the temporal variability and changes in snow cover duration and the average snow depth from December to April in the Pyrenees at 1500 and 2100 m a.s.l. for the period 1958–2017. This is the first such analysis for the entire mountain range using SAFRAN-Crocus simulations run for this specific purpose. The SAFRAN-Crocus simulations were evaluated for the period 1980–2016 using 28 in situ snow depth data time series, and for the period 2000–2017 using MODIS observations of the snow cover duration. Following confirmation that the simulated snow series satisfactorily reproduced the observed evolution of the snowpack, the Mann-Kendall test showed that snow cover duration and average depth decreased during the full study period, but this was only statistically significant at 2100 m a.s.l. The temporal evolution in the snow series indicated marked differences among massifs, elevations, and snow variables. In general, the most western massifs of the French Pyrenees underwent a greater decrease in the snowpack, while in some eastern massifs the snowpack did not decrease, and in some cases increased at 1500 m a.s.l. The results suggest that the trends were consistent over time, as they were little affected by the start and end year of the study period, except if trends are computed only starting after 1980, when no significant trends were apparent. Most of the observed negative trends were not correlated with changes in the atmospheric circulation patterns during the snow season. This suggests that the continuous warming in the Pyrenees since the beginning of the industrial period, and particularly the sharp increase since 1955, is a major driver explaining the snow cover decline in the Pyrenees.

**Keywords:** Snow, Trends, Weather Types, Pyrenees

## 1. Introduction

Seasonal snow is essential for most environmental, hydrological, and geomorphological processes in mountain areas. The insulation effect whereby snow cover protects the underlying substrate from atmospheric temperatures directly controls the thermal regime of soils, and determines the phenological cycles of plants and animals living at high elevations (Kankaanpää *et al.*, 2018; Wang *et al.*, 2018; Serrano *et al.*, 2019). The

snowpack also acts as a natural reservoir of water, formed during the cold season from the accumulated precipitation. The water is released during the melt period, and this governs the timing of river flows and also provides mountain basins with a greater temporal regularity compared with areas dominated by liquid precipitation (Barnett et al. 2005; López-Moreno et al. 2017; Sproles et al. 2018). The state of the snow cover also has clear implications for local communities, as it is a source of major hazards including avalanches, heavy snowfall events, and rain on snow events that affect the security of people and infrastructure (Eckert *et al.*, 2013; Surfleet and Tullos, 2013; Navarro-Serrano and López-Moreno, 2017). In addition, its reliable presence is the main factor for various winter tourism activities that have become the primary source of economic income in many mountain regions worldwide (Gilaberte-Búrdalo *et al.*, 2014; Spandre *et al.*, 2019).

There is growing concern about the consequences of ongoing climate warming on the mountain snow cover, evident in the growing body of published research devoted to identifying changes in the duration and thickness of snowpack in various regions of the world (Hock et al., in press), including the Mediterranean mountains (García-Ruiz *et al.*, 2011; Marchane *et al.*, 2015) and the Alps (Klein et al., 2016; Marty et al., 2017, Schöner *et al.*, 2019). Many studies have involved sensitivity analyses and predictions of the impact of various climate scenarios on the snowpack in coming decades (Rasouli *et al.*, 2014, 2019; Musselman *et al.*, 2017, Verfaillie et al., 2018, Beniston et al., 2018). However, the study of past snowpack trends is highly constrained by the generally limited number of long-term measurements at high elevation sites, where the snowpack plays the most important role (Hock et al., in press). In addition, the stations providing long-term observations are generally unevenly distributed, which makes it difficult to obtain data at regional scales or for entire mountain ranges (Rohrer *et al.*, 2013). Another difficulty in snow trend analyses comes from the very high interannual and decadal variability commonly evident in snowpack series (Wegmann *et al.*, 2017); such data can only be adequately analyzed from multidecadal snow series (Mankin and Diffenbaugh, 2015). Successful analyses have only been achieved based on data from very dense networks having long-term observations, including that recently published for Switzerland and Austria (Schöner *et al.*, 2019). The European Alps are arguably the European mountain region richest in terms of data availability, and where these type of

studies have been conducted (Laternser and Schneebeli 2003; Marty 2008; Morán-Tejeda et al. 2013; Marke *et al*., 2018; Schöner et al. 2019; Marty et al., 2017). Studies on the evolution of snow cover based on remote sensing data have provided information on the regional temporal variability of snow cover and snow line elevation, but their limited temporal extent prevents robust assessment of significant trends (Bormann *et al.*, 2018). An alternative to the use of observed snow series is the use of simulated snow series driven by atmospheric reanalyses or observations (Alonso-González et al. 2019; van Pelt et al. 2016; Durand et al. 2009; Mote et al., 2018; Marke et al. 2018). Although the results can differ from those based on snow observations, they have been shown to adequately reproduce the interannual evolution of the duration and thickness of the snowpack (Martin and Etchevers 2005; Durand et al. 2009; Alonso-González et al. 2018). Thus, they can provide long-term and spatially distributed information on the snow cover over large areas, enabling regional assessment of snow changes despite limited availability of direct snow cover observational data.

The main objective of this study is to analyze the temporal evolution of snow cover duration and average snow depth in the Pyrenees and to assess to which extent the variability is controlled by regional atmospheric circulation. This work also aims to identify spatial differences in the temporal evolution of snow depth series, and to assess the temporal consistency of the trends when different study periods are considered. We used simulated snow series from the combined application of the atmospheric reanalysis SAFRAN and the snowpack model Crocus for the period 1958–2017. The temporal consistency of the trends in the snow series was tested by analyzing the dependence of the trend patterns on the chosen start and end year of the study time series. We then investigated changes in the frequency of weather types (synoptic situations) over the Pyrenees during each analyzed snow season to assess whether the detected trends were dependent on shifts in atmospheric circulation patterns, which are subject to natural variability, or whether the trends could be attributed to other drivers, in particular the observed regional climate warming. This is relevant because recent temperature data compiled by weather agencies in France, Spain, and Andorra have shown that the Pyrenees has undergone an increase in annual temperature of 1.3°C since 1955 (Pyrenean Observatory of Climate Change, 2019).

## 2. Study area

The Pyrenees is the northern limit of the Iberian Peninsula and creates a natural border between Spain and France. It extends from west to east over 400 km from the Atlantic Ocean to the Mediterranean Sea, and is 150 km at its widest point (along a north–south axis) in the central area (Figure 1). It is a transboundary mountain area, including the territory of three countries: France, Spain, and Andorra. The Pyrenean headwaters include the main tributaries of large rivers including the Ebro River, which flows to the Mediterranean Sea, and the Garonne River, which flows to the Atlantic Ocean. The Pyrenean range is a key source of runoff meeting the water demands of 7 million people and supplying hydropower and large irrigation areas on both sides of the mountain range. The highest peaks of the Pyrenees are in the central and eastern parts of the range, where more than 150 peaks exceeding 3000 m occur (the maximum elevation is reached in the Aneto peak: 3404 m a.s.l.), and large areas are above 2000 m a.s.l.

-Figure 1-

The climate of the Pyrenees is highly variable in the east–west direction, as it reflects the transition from Atlantic to Mediterranean climates. There is also a marked climatic difference between the northward and southward slopes along the main axis of the range, with the former being markedly more humid. Annual precipitation ranges from 600 mm in the dryer areas in the eastern part of the Spanish Pyrenees, to up to 3000 mm in the most humid parts of the western Pyrenees and on slopes facing north and northwest in the most elevated central massifs (Serrano-Notivoli *et al.*, 2017). The elevation of the annual 0°C isotherm ranges from 2700 to 3000 m a.s.l. (López-Moreno et al. 2019), while the winter 0°C isotherm is located at approximately 1500 m a.s.l., which is the approximate limit for the seasonal snowpack during the coldest months of the year (López-Moreno 2005; Gascoin et al. 2015). Above 2000 m a.s.l. the duration of snowpack often exceeds six months (López-Moreno et al. 2017; Gascoin et al. 2015). Snow is a key resource for the region; López-Moreno and García-Ruiz (2004) estimated that the snowmelt contributes > 40% of the spring runoff for the Ebro headwaters, and noted that it is a major complement to dams for synchronizing water demand and water availability, mainly for agriculture and hydropower production. The snowpack has been

also reported to have a significant influence on forest growth and health in several Pyrenean areas at 1300–2300 m a.s.l. (Sanmiguel-Vallelado *et al.*, 2019). There are more than 30 ski resorts in the Pyrenees, serving a mean annual population of 5 million skiers, and is the major source of income for many Pyrenean valleys (Gilaberte-Búrdalo *et al.*, 2017). The communities involved depend directly on the quantity and duration of the snowpack, and there is growing concern about its reliability given the climate warming projections for the coming decades (Pons et al. 2015), and the extent to which snowmaking and other snow management techniques will be able to address the increasing snow scarcity suggested by climate change scenarios (Spandre *et al.*, 2019).

## 3. Methods

### 3.1 SAFRAN Crocus simulations

SAFRAN is a reanalysis system combining in-situ meteorological observations, remotely sensed cloud cover information and large scale meteorological predictions, in order to provide a consistent and gap-free estimate of the meteorological conditions in mountainous regions, here the Pyrenees (Durand et al., 2009). The Pyrenees are decomposed in 23 regions (shown in Figure 1) so called "massifs", considered climatologically homogeneous, within which SAFRAN provides meteorological information at hourly time resolution and by elevation steps of 300 m elevation. In addition, SAFRAN can also provide meteorological information with adjustments of temperature and radiations considering the exact elevation of a given location and its surrounding topographic masks (but the spatial scale of the meteorological analysis remains the massif). In this work, SAFRAN data are used for all massifs in the Pyrenees for 300 m elevations bands on flat terrain. Model simulations used in this study span the time period from 1958 to 2017. This corresponds to a version almost identical to the dataset available made available by Vernay et al., (2019). The last corrections made before the publication of this dataset are sufficiently minor to not modify the conclusions of this study.

The SAFRAN meteorological reanalysis was used to force the detailed snowpack model Crocus (Vionnet et al., 2012) which provides estimates of snow cover depth, amount

and various other properties using a multi-layer modelling approach. In this study, we used the spatial configuration for Crocus forced by SAFRAN (massifs/elevations and corresponding to observation stations) used operationally in France in support for avalanche forecasting as described in Morin et al. (2020).The SAFRAN-Crocus simulations were also used in the gap filling procedure of 28 long-term snow observation series used in the model evaluation process (section 3.2). For this purpose, at observation stations, observed snow depth data were used to correct the simulated snow depth and re-initialize the following simulations, with the same method as applied by Revuelto et al. (2016) with snow depth data from a Terrestrial Laser Scanner. Here, this method was implemented on a daily basis, i.e. simulations were stopped every day, snow depth was compared to observed snow depth, and in the case were snow depth values existed, the observed snow depth value was used to adjust the thickness of all simulated snow layers in Crocus so that the snow depth values match, keeping constant the other state variables of each layer (density, temperature, liquid water content, microstructure properties). In cases where snow observations were missing, Crocus prognostic variables were left unchanged. In the case where observations indicated 0, the Crocus snowpack was removed, and in the case where Crocus predicted 0 snow depth while observations indicated non-zero values, Crocus was reinitialized with a generic, snowpack structure matching the observed snow depth. This typical snowpack structure was generated, using a Crocus model run driven by a SAFRAN forcing file and stopped when the snow depth reached approximately 5 and 50 cm, respectively. Depending on the observed snow depth, either of these two files were used, in order to initialize Crocus with a snowpack structure which is consistent with the corresponding snow depth. While this method of direct insertion is not as advanced as proper data assimilation, it allows for gap-filling, taking advantage of the fact that the snow cover evolves with a large auto-correlation in time and that the SAFRAN-Crocus model chain already provides an appropriate estimate of the daily snow cover evolution for trend analysis, based on previous studies (Lafaysse et al., 2013, Durand et al., 2009, Spandre et al., 2019). Meanwhile, this method allowed us to detect and remove outliers in observed snow depth time series, warranting further investigations (combining other data sources, such as temperature, precipitation and wind speed), where the observed snow cover deviates strongly from the simulated one. The outcome of this method is a gap-filled observed snow depth time series, corresponding exactly to the observed

values when they are present, and filled with physically consistent values in the case of data gaps, including during the melt season at the end of the winter, when many manual observations are not performed anymore due to the seasonal closure of ski resorts where the observations are carried out by specially trained ski patrollers. Figure 2 shows four examples of simulated snow series with SAFRAN Crocus approach before (Sims) and after applying the re-initialization procedure explained in this section (Sims-Assim).

-Figure 2-

3.2 Evaluation of SAFRAN Crocus simulations

Before doing the trend analysis, the ability of SAFRAN Crocus to reproduce the annual average snow depth (HS) and annual snow cover duration (SCD) was specifically evaluated for this study.

The simulated HS was compared to the HS obtained from reconstructed snow depth observations at 28 long term stations over the period 01 August 1979 to 31 July 2016 (hereinafter referred to as "station HS"). These reconstructed snow depth series were considered as "ground truth" since these reconstructed time series do not differ from the observations when there are observations, and although the method introduces some artificial errors correlations during the reconstructed periods (after the closure of a ski resort performing observations, the error is constant by construction as the melting rates are identical in the simulation and in the reference). The station HS dataset was made from stations which have a record longer than 20 years and whose average missing data fraction in the daily series is greater than 60% during the months December to April (DJFMA). From these gap-free station series, the mean annual snow depth was computed as the mean snow depth during the months DJFMA. The advantage of using this reconstructed station HS instead of the raw HS data is that it enables to compute a mean annual snow depth without having to deal with unevenly distributed data gaps. HS values at a station were compared to HS value in the corresponding massif and elevation band.

The simulated annual SCD was evaluated using a daily gap-filled snow cover

climatology from MODIS snow products MOD10A1.005 and MYD10A1.005 (Gascoin et al., 2015). The MODIS dataset covers the period 01 August 2000 to 31 July 2016. For a given hydrological year, the SCD was defined by pixel as the total number of days labeled as snow. The same metric was extracted from the SAFRAN-Crocus reanalysis by computing the number of days with a mean daily snow depth higher than 15 cm. We chose 15 cm because it is the optimal threshold identified by Gascoin et al. (2015) from the comparison of MODIS snow products with in situ measurements in the Pyrenees. For a given massif, SAFRAN-Crocus provides one value of the annual snow cover duration by elevation band (only the flat slope class was considered). However, MODIS provides one value per 500 m pixel, which means that there is an ensemble of SCD values to compare to this SAFRAN-Crocus SCD value. Hence, the SRTM DEM was used to aggregate all annual SCD values from MODIS pixels by massif and elevation band using the median.

### 3.3 Statistical analysis

From the daily series of snow depth we calculated the annual duration of the snow cover as the number of days from October to September of the following year, and the average snow depth was calculated for the period from December to April, considered typically as the period where a seasonal snowpack can be found in the Pyrenees over 1500 m a.s.l. (López-Moreno et al., 2005). We selected for further analysis those series corresponding to elevations of 1500 and 2100 m a.s.l. The former was selected because it is considered an elevation where the seasonal snowpack is normally present in all the massifs, while at lower elevations the snowpack is ephemeral with multiple melting events during winter (López-Moreno, 2005). Furthermore, the lowest elevation of many ski areas is at approximately 1500 m, which makes it a relevant elevation band on a winter tourism perspective (Pons *et al.*, 2012). At 2100 m a.s.l. the snowpack is much thicker and longerlasting, representing a significant water resource for the Pyrenees. Although snow is usually more abundant at higher elevations, the area at elevations of 2400 m a.s.l. or higher is relatively small within the Pyrenean range, or absent in the westernmost massifs. The average values for the 23 massifs, for each elevation band

considered, were considered as the regional series for the Pyrenees. A varimax rotated principal component analysis (PCA) (Abdi, 2003; Hannachi, 2004) was then performed for each variable (snow cover duration and average snow depth for DJFMA) and elevation (1500 and 2100 m a.s.l.) to facilitate grouping of massifs (those exhibiting the maximum correlation with each PC) having a similar interannual evolution of the snow series.

The nonparametric Mann-Kendall (MK) test was used to detect trends in the temporal series (Mann, 1945; Kendall, 1948), using a significance level of $p < 0.05$. The MK trend test is rank-based, so it can also be applied to series that do not follow a normal distribution or contain outliers (Cunderlik and Ouarda, 2009). The Kendall's tau statistic (range −1 to 1) was used to quantify the strength of the trends. We checked that the series were free of lag-1 autocorrelation, and determined that prewhitening of the series was not necessary (Yue and Wang, 2002). To check the temporal coherence of the detected trends we calculated a matrix of all possible combinations of starting and ending years (minimum of 20 years length) in the series for each snow variable and the corresponding elevation, based on those massifs that showed the highest correlation with the groups that exhibited major trends, as identified by the PCA. This procedure enabled us to assess whether the identified trends were dependent on the specific study period considered in our study, or were robust and independent of the interannual variability of the series.

### 3.4 Weather type classification

The daily synoptic conditions over the Pyrenees during the study period were calculated using the objective classification method of Jenkinson and Collison (1977), which has been widely applied in climatological studies (see the review of Navarro-Serrano and López-Moreno 2017). The method uses a grid of 16 points of atmospheric sea level pressure centered in the central Pyrenees (42ºN, 1ºE) and spaced at 5° intervals, derived from NCEP/NCAR reanalysis (Basnet and Parker, 1997). This enabled calculation of the direction and vorticity of the geostrophic flow, which facilitated classification of each day as cyclonic (C) or anticyclonic (A), and into directional (8) and hybrid (16) types. Hybrid types were removed using the approach used proposed by Trigo and DaCamara (2000). The number of occurrences of each weather type recorded each year

303 from December to April was summed, and the 10 remaining series (C, A, and 8
304 directions) were reduced using a varimax rotated PCA, as done for the snow series.

305

306 **4. Results**

307 4.1 Evaluation of the simulated snow series

308 A good correlation (Spearman R = 0.87) was found between the reconstructed mean
309 annual observed snow depth (station HS) and the simulated HS (Fig. 3A); the difference
310 was very small between the two datasets (8 cm). It is important to note that
311 discrepancies between observations and simulations are not only explained by
312 modelling errors but also by the unresolved horizontal intra-massif variability. The
313 performance of the model in relation to snow cover duration obtained from MODIS
314 images was also good (R = 0.96 and a difference of 20.6 days; Fig. 3B).

315

316 -Figure 3-

317

318 4.2 Trend analysis

319 Figure 4 (A and B) shows the temporal evolution of the regional series for the 23
320 massifs in the Pyrenees, calculated as the annual average snow cover duration at 1500
321 and 2100 m a.s.l. and the average snow depth from December to April. The snow cover
322 duration at 1500 m a.s.l. showed large interannual variability, because there were years
323 when the snow did not last more than 1.5 months, while in other years the snow cover
324 duration exceeded three months. Over the period 1958–2017 the series showed a
325 negative trend, but this was not statistically significant ($p > 0.05$). At 2100 m a.s.l. the
326 snow cover duration was also highly variable, with a duration in most years ranging
327 from 4 to 6 months, but the long-term negative trend was statistically significant ($p <$
328 0.05). Very similar results were found for the average (DJFMA) snow depth at 1500
329 and 2100 m a.s.l. (Fig. 4 C and D). At both elevations the snow depth showed high
330 interannual variability, in most years ranging from 10 to 40 cm at 1500 m a.s.l., and

331 from 60 to 120 cm at 2100 m a.s.l.. Both series showed negative long-term trends, but
332 this was only statistically significant ($p < 0.05$) for 2100 m a.s.l.

333

334 -Figure 4-

335

336 The results for the regional series shown in Figures 4 did not demonstrate differences in
337 interannual evolution that occurred among the 23 massifs. To assess the variability in
338 snow evolution in the Pyrenees, the PCA classified two main groups of massifs
339 according their similar temporal evolution of snow cover duration at 1500 m a.s.l. (Fig.
340 5A); these explained 79% of the variance. Principal component 1 (PC1) was highly
341 correlated with the snow cover duration in the central and western Pyrenees (Fig. 5B).
342 Negative trends clearly dominated in these massifs, especially those located in the
343 westernmost part of the French Pyrenees. Principal component 2 (PC2) reflected the
344 snow cover duration in the eastern massifs, where no trend or a positive trend was
345 apparent. Among the 23 massifs, eight showed statistically significant ($p < 0.05$)
346 negative trends, and two showed statistically significant positive trends.

347 For 2100 m a.s.l. the PCA analysis identified four groups that explained 85% of the
348 observed variance in the interannual evolution of snow cover duration at this elevation
349 (Fig. 5C). PC1 represented the western massifs of the French Pyrenees and the Navarra
350 region on the Spanish side (Fig. 5D). Patterns similar to PC2 2 were found for the
351 eastern massifs; PC3 in central Pyrenees and the PC4 represents some massifs in
352 transition from west to central Pyrenees. Negative Kendall's tau values were found for
353 most of the massifs; 13 of the 23 showed statistically significant negative trends ($p <$
354 0.05), and none exhibited a statistically significant positive trend.

355

356 -Figure 5-

357

The interannual evolution of average snow depth at 1500 m a.s.l. in the 23 massifs was reflected by three principal components that explained 86% of the observed variance (Fig. 6A). PC1 represented the western and central massifs of the Pyrenees, which had generally negative trends, especially in the westernmost French massifs (Fig. 6B); PC2 and PC3 represented massifs located to the east. The majority had Kendall's tau values close to 0, but several positive coefficients were found for the easternmost part. Overall, five of the 23 massifs showed statistically significant negative trends ($p < 0.05$), and two showed statistically significant positive trends ($p < 0.05$). The average snow accumulation (DJFM) at 2100 m a.s.l. was also classified into three PCA groups that explained 89% of the observed variance (Fig. 6C). PC1 represented the western French massifs, which showed marked negative trends (Fig. 6D), PC2 represented the eastern massifs, and PC3 represented the western Spanish Pyrenees and the central French Pyrenees. Negative Kendall's tau values also dominated the massifs represented by PC2 and PC3, and overall 14 of the 23 massifs showed statistically significant negative trends ($p < 0.05$), and no massif showed a statistically significant positive trend.

- Figure 6-

The observed negative trends in snow cover duration and snow depth, found particularly for the western Pyrenees, showed marked temporal consistency and little dependence on the study period. The three plots in Figure 7 show that there was a clear dominance of pairs of starting and ending years showing a statistically significant decrease. Only the upper right portions of the matrices lack any statistically significant trend, or showed a change in the sign of the Kendall's tau values. Thus, trend analyses starting from 1957 to 1980 and finishing in recent years showed statistically significant negative trends that were not affected by decadal fluctuations of the snowpack. However, for series starting after 1980 there were no statistically significant trends, and the Kendall's tau coefficients were positive, as can be seen from the temporal evolution of snow depth and duration, shown in the lower right corner of each plot.

-Figure 7-

4.3. Atmospheric circulations patterns and their impacts on snow trends

The winter (DJFMA) frequency for the eight weather types classified for the Pyrenees was simplified to four groups of years (PCA; Table 1) that explained 84% of the observed variance. PC1 was highly correlated with years characterized by a low frequency of anticyclonic conditions, and a high frequency of advections from the southwest and west. PC2 was highly correlated with years having a high frequency of advections from the east and northeast, and a low frequency from the northwest. PC3 was characterized by a low frequency of cyclonic conditions and a high frequency of advections from the north. PC4 was characterized by a high frequency of advections from the south and a low frequency from the northwest.

- Table1-

Only PC1 showed a statistically significant negative trend (Mann-Kendall tau = –0.53; $p < 0.05$), which indicated an increase in the frequency of anticyclonic days and a decrease of advections from the northwest and west. The factorial scores for the other three PCs did not shown significant changes (Figure 8), with Mann-Kendall tau values very close to 0. Correlation analysis of PC1 with the groups discriminated according to the interannual evolution of snow indices only showed statistically significant correlations with Group 3 (average depth at 2100 m a.s.l.; $r = 0.57$) and Group 1 (snow cover duration at 1500 m a.s.l.; $r = 0.29$).

-Figure 8-

## 5. Discussion

This study showed that the Crocus snow cover model driven by the atmospheric SAFRAN model satisfactorily reproduced the snow evolution over the Pyrenees during the period 1980–2017, enabling the first assessment of long-term trends (1958-2017) for this entire mountain range in the absence of comprehensive observational data. This method has previously been used and evaluated in a study in the French Alps (Durand *et al.*, 2009), although it is known that local discrepancies between simulated and observed trends are possible (Lafaysse et al, 2011, Verfaillie et al, 2018). Indeed, simulated trends are affected by various sources of temporal heterogeneity along the simulation period. First, the surface meteorological observations assimilated by the SAFRAN reanalysis have changed over time and it is known that these heterogeneities can significantly affect local trends (Vidal et al, 2010). This effect is expected to be reduced when considering larger scale trends, as done in this paper when considering the whole Pyrenees mountain range. Then, the guess of the reanalysis is also heterogeneous over time. The two main heterogeneities are due to the onset of satellite observations in the 1980s known to be responsible for temporal breaks in ERA-40 reanalysis (Sterl, 2004), and the switch from ERA-40 reanalysis to ARPEGE operational analyses for years after 2001. Although these limitations can not be completely removed, it can be reduced in future works by updating the SAFRAN reanalysis by using more recent large scale reanalyses for the guess, such as ERA5.

Regional series for the Pyrenees revealed declining snow cover duration and average snow accumulation during the study period, but the trends were only statistically significant at 2100 m a.s.l., but not at 1500 m. This finding appears counterintuitive, as previous studies have reported greater sensitivity of the snowpack to climate warming in areas near the 0°C isotherm during the snow season compared with colder areas (Pierce and Cayan 2013; Marty et al. 2017). The most likely explanation for our results is the different rates of climate warming reported for the Pyrenees on a seasonal basis. The report recently published by the Pyrenean Observatory of Climate Change (OPCC, 2019) and Serrano-Notivoli et al. (2019) notes that warming rates since 1955 have been lower during winter months (+0.1°C per decade; $p > 0.05$) and greater in spring and fall (+0.3 and +0.2°C, respectively; $p < 0.05$). A similar seasonal pattern was reported by Pérez-Zanón et al. (2017) for the period 1970–2013. No statistically significant change in precipitation occurred during the study period (OPCC, 2019), and its interannual

446 evolution has been found to be closely related to interannual variability in the frequency
447 of weather types (Buisan *et al.*, 2016). In this climate context, snowpacks that lasts after
448 March (the case for the snowpack at 2100 m a.s.l.) are expected to show stronger trends
449 than snowpacks restricted to the colder winter months (the case for the snowpack at
450 1500 m a.s.l.). This consideration has not yet been taken into account in interpreting the
451 response of snowpacks to climate warming. The same explanation applies to the evident
452 decrease in snow cover duration, affecting to the start and end of the snow cover, and
453 accumulation in the westernmost massifs and massifs to the north of the range
454 compared with the remainder of the Pyrenees. Apprndix T1 shows that the snow lasts
455 longer on these massifs, and hence is exposed to the higher warming rates observed
456 outside of the coldest months.

457 Some of the significant trends found in this study can also be related to an increase in
458 the occurrence of anticyclonic conditions and a decrease in advections from the west
459 and south west, as evidenced by the statistically significant decrease of PC1. PC1 was
460 clearly linked to the positive evolution of the North Atlantic Oscillation index (NAOi),
461 as previously shown for the Iberian Peninsula by López-Moreno and Vicente-Serrano
462 (2007). In that study it was noted that the interannual evolution of the snowpack in the
463 central Spanish Pyrenees is controlled by the NAO, especially at elevations above 2000
464 m. Thus, the negative trend in snow accumulation at several observatories in the study
465 area can be explained by such changes in atmospheric circulation. Alonso-González et
466 al. (submitted) recently analyzed the effect of the NAO on the snowpack over the entire
467 Iberian Peninsula, and showed that it only has an evident effect in this portion of the
468 Pyrenees, and its effect is very limited or nonexistent in the northern massifs and at low
469 elevations throughout the entire range. Thus, many of the negative trends reported in
470 this study cannot be directly explained by changes in atmospheric circulation patterns,
471 as the other patterns identified did not show any significant trend. In the absence of
472 clear trends for precipitation, this finding strongly suggests that the main driver of the
473 decline in the snowpack in the Pyrenees is long-term climate warming.

474 The major trends in the Pyrenees during the study period seemed to be consistent over
475 time and not significantly affected by the selected start and end years when long-term
476 time series were considered. However, for analysis periods starting after 1980, no
477 significant trends in the snowpack were found. A very similar finding has been reported

for the Swiss and Austrian Alps, where only small changes since the end of the 1980s have been observed (Marty, 2008; Schöner *et al.*, 2019). This result illustrates the importance of using sufficiently long observation records when assessing trends of snow series (Fassnacht and Hulstrand, 2015).

For the Pyrenees, the temporal series of temperature evolution in the evolution provides an explanation (OPCC, 2019). The temperature increase since 1955 is mostly evident in the stark contrast between the cold decades of the 1960s and 1970s, and the much warmer following decades. However, the temperature trends after 1980 have been weaker or nonexistent (López-Moreno et al., 2019). This explains why some studies using snow data for the Spanish Pyrenees since 1986 have found no trends in the snowpack (Buisan et al. 2015; Morán-Tejeda et al. 2017); for this specific part of the Pyrenees this finding is reinforced by the relatively high frequency of winters having negative NAOi values (Añel et al. 2014; Buisan et al. 2016), which is associated with frequent humid conditions in the massifs located southwards.

## 6. Conclusions

The main findings of this work can be summarized as follows:

1. SAFRAN-Crocus satisfactorily reproduced the main space and time variations in the snow cover in the Pyrenees from 1980 to 2017 based on in-situ and remote sensing observations, providing confidence in the trends in simulated values from 1958 to 2017 although the temporal homogeneity of the data is not fully guaranteed.

2. In general, the snowpack decreased during the period 1958–2017, and the decline has been clearer at 2100 m a.s.l. This is consistent with the climate trends detected in the study, as warming during the study period was greater in fall and spring compared with winter (when the snowpack is limited at 1500 m).

3. There was marked spatial variability among massifs, and this differed for the two analyzed indices (snow cover duration and average snow depth DJFMA) and the two analyzed elevation bands (1500 and 2100 m a.s.l.). Overall, the western Pyrenees showed the most statistically significant decline in the snowpack.

4. Most of the significant trends detected showed high temporal consistency during the study period, and low dependence on the period selected, provided this was sufficiently long. The results suggest that only trends for snow accumulation at 2100 m a.s.l. in the central Pyrenees are linked to changes/variability in atmospheric circulation patterns (increase in the NAOi).

5. This study highlights the need for using long-term records and evenly distributed spatial data in the analysis of snow trends.

**Acknowledgements.** This study was funded by the project CLIMPY: 'Characterization of the evolution of climate and provision of information for adaptation in the Pyrenees' (FEDER-POCTEFA); and HIDROIBERNIEVE (CGL2017-82216-R), from the Spanish Ministry of Science, Innovation and Universities. CNRM/CEN belongs to LabEX OSUG@2020. This study benefitted from funding from the European Union's Horizon 2020 research and innovation programme under grant agreement No 730203.

## REFERENCES

Abdi H. 2003. Factor Rotations in Factor Analyses. Encyclopedia of social sciences research methods. M. Lewis-Beck, A. Bryman, T. Futimg (Eds.), Encyclopedia for Research Methods for the Social Sciences, Sage Publications; Publications, Thousand Oaks, CA .

Añel JA, López-Moreno JI, Friederike O, Vicente Serrano SM., Schaller N, Massey N, Buisán ST, Allen MR 2014. The extreme snow accumulation in the western Spanish Pyrenees during winter and spring 2013. Bulletin of the American Meteorological Society, 95(9): S73-S76. http.hdl.handle.net/10261/110100.

Alonso-González E, López-Moreno JI, Gascoin S, García-Valdecasas Ojeda M, Sanmiguel-Vallelado A, Navarro-Serrano F, Revuelto J, Ceballos A, Esteban-Parra MJ, Essery R. 2018. Daily gridded datasets of snow depth and snow water equivalent for the

534 Iberian Peninsula from 1980 to 2014. Earth Syst. Sci. Data, 10(1): 303–315.
535 https://doi.org/10.5194/essd-10-303-2018.

536 Alonso-González E, López-Moreno JI, Navarro-Serrano F, Sanmiguel-Vallelado
537 A, Revuelto J, Domínguez-Castro F, Ceballos A. 2019. Snow climatology for the
538 mountains in the Iberian Peninsula using satellite imagery and simulations with
539 dynamically downscaled reanalysis data. International Journal of Climatology 40 (1):
540 477-491. https://doi.org/10.1002/joc.6223.

541 Alonso-González E, López-Moreno JI, Navarro-Serrano FM, Revuelto J. 2020
542 Impact of North Atlantic Oscillation on the Snowpack in Iberian Peninsula
543 Mountains. Water 12: 105. https://doi.org/10.3390/w12010105

544 Barnett TP, Adam JC, Lettenmaier DP. 2005. Potential impacts of a warming
545 climate on water availability in snow-dominated regions. Nature, 438: 303-309.
546 https://doi.org/10.1038/nature04141

547 Beniston M, Farinotti D, Stoffel M, Andreassen LM, Coppola E, Eckert N,
548 Fantini A, Giacona F, Hauck C, Huss M, Huwald H, Lehning M, López-Moreno J.I,
549 Magnusson J, Marty C, Morán-Tejéda E, Morin S, Naaim M, Provenzale A, Rabatel, A,
550 Six D, Stötter J, Strasser U, Terzago S,, Vincent C. 2018. The European mountain
551 cryosphere : a review of its current state, trends, and future challenges. The Cryosphere,
552 12: 759-794. https://doi.org/10.5194/tc-12-759-2018.

553 Bormann KJ, Brown RD, Derksen C, Painter TH. 2018. Estimating snow-cover
554 trends from space. Nature Climate Change, 8(11): 924–928.
555 https://doi.org/10.1038/s41558-018-0318-3.

556 Buisan ST, López-Moreno JI, Saz MA, Kochendorfer J. 2016. Impact of weather
557 type variability on winter precipitation, temperature and annual snowpack in the
558 Spanish Pyrenees. Climate Research, 69(1): 79-92. https://doi.org/10.3354/cr01391.

559 Buisan ST, Saz MA, López-Moreno JI. 2015. Spatial and temporal variability of
560 winter snow and precipitation days in the western and central Spanish Pyrenees.
561 International Journal of Climatology, 35(2): 259-274. https://doi.org/10.1002/joc.3978.

562 Cunderlik JM, Ouarda TBMJ. 2009. Trends in the timing and magnitude of
563 floods in Canada. Journal of Hydrology, 375(3–4): 471–480.
564 https://doi.org/10.1016/J.JHYDROL.2009.06.050.

565 Durand Y, Giraud G, Laternser M, Etchevers P, Mérindol L, Lesaffre B. 2009.
566 Reanalysis of 47 Years of Climate in the French Alps (1958-2005): Climatology and
567 Trends for Snow Cover. Journal of Applied Meteorology and Climatology, 48: 2487–
568 2512. https://doi.org/10.1175/2009JAMC1810.1.

569 Eckert N, Keylock CJ, Castebrunet H, Lavigne A, Naaim M. 2013. Temporal
570 trends in avalanche activity in the French Alps and subregions: from occurrences and
571 runout altitudes to unsteady return periods. Journal of Glaciology, 59(213): 93–114.
572 https://doi.org/DOI: 10.3189/2013JoG12J091.

573 Fassnacht SR, Hultstrand M. 2015. Snowpack variability and trends at long-term
574 stations in northern Colorado, USA. Proc. IAHS 371: 131–136.
575 https://doi.org/10.5194/piahs-371-131-2015.

576 García-Ruiz JM, López-Moreno JI, Vicente-Serrano SM, Lasanta-Martínez T,
577 Beguería S. 2011. Mediterranean water resources in a global change scenario. Earth-
578 Science Reviews, 105(3–4). https://doi.org/10.1016/j.earscirev.2011.01.006.

579 Gilaberte-Búrdalo M, López-Martín F, Pino-Otín MR, López-Moreno JI. 2014.
580 Impacts of climate change on ski industry. Environmental Science and Policy, 44: 51-
581 61. https://doi.org/10.1016/j.envsci.2014.07.003.

582 Gilaberte-Búrdalo M, López-Moreno JI, Morán-Tejeda E, Jerez S, Alonso-
583 González E, López-Martín F, Pino-Otín MR. 2017. Assessment of ski condition
584 reliability in the Spanish and Andorran Pyrenees for the second half of the 20th century.
585 Applied Geography, 79: 127-142. https://doi.org/10.1016/j.apgeog.2016.12.013.

586 Hannachi A. 2004. A primer for EOF analysis of climate data. Conference
587 Proceedings. Department of Meteorology, University of Reading.

588 Hock R, Rasul G, Adler C, Cáceres B, Gruber S, Hirabayashi Y, Jackson M,
589 Kääb A, Kang S, Kutuzov S, Milner A, Molau U, Morin S, Orlove B, Steltzer H. 2019:

590 High Mountain Areas. In: IPCC Special Report on the Ocean and Cryosphere in a
591 Changing Climate [H.-O. Pörtner, D.C. Roberts, V. Masson-Delmotte, P. Zhai, M.
592 Tignor, E. Poloczanska K. Mintenbeck, A. Alegría, M. Nicolai, A. Okem, J. Petzold, B.
593 Rama, N.M. Weyer (eds.)].

594 Kankaanpää T, Skov K, Abrego N, Lund M, Schmidt NM, Roslin T. 2018.
595 Spatiotemporal snowmelt patterns within a high Arctic landscape, with implications for
596 flora and fauna. Arctic, Antarctic, and Alpine Research, 50(1): e1415624.
597 doi.org/10.1080/15230430.2017.1415624.

598 Kendall MG. 1948. Rank correlation methods. Rank correlation methods.
599 Griffin: Oxford, England.

600 Klein G, Vitasse Y, Rixen C, Marty C, rebetez M. 2016. Shorter snow cover
601 duration since 1970 in the Swiss Alps due to earlier snowmelt more than to later snow
602 onset. Climatic Change, 139**:** 637–649. https://doi.org/10.1007/s10584-016-1806-y

603 Lafaysse M, Hingray B, Etchevers P, Martin E, Obled C. 2011. Influence of
604 spatial discretization, underground water storage and glacier melt on a physically based
605 hydrological model of the Upper Durance River basin. Journal of Hydrology, 403: 116
606 - 129. https://doi.org/10.10016/j.hydrol.2011.03.046

607 Laternser M, Schneebeli M. 2003. Long-term snow climate trends of the Swiss
608 Alps (1931–99). International Journal of Climatology, 23(7): 733–750.
609 https://doi.org/10.1002/joc.912.

610 López-Moreno JI. 2005. Recent variations of snowpack depth in the central
611 Spanish Pyrenees. Arctic, Antarctic, and Alpine Research, 37(2): 253-260.
612 https://doi.org/10.1657/1523-0430(2005)037.

613 López-Moreno JI, Alonso-González E, monserrat o, Del Río LM, Otero J,
614 Lapazaran J, Luzi G, Dematteis N, Serreta A, Rico I, Serrano-Cañadas E, Bartolomé M,
615 Moreno A, Buisan S, Revuelto J. 2019. Ground-based remote-sensing techniques for
616 diagnosis of the current state and recent evolution of the Monte Perdido Glacier,

617 Spanish Pyrenees. Journal of Glaciology, 65(249): 85–100. https://doi.org/DOI:
618 10.1017/jog.2018.96.

619 López-Moreno JI, García-Ruiz JM. 2004. Influence of snow accumulation and
620 snowmelt on streamflow in the central Spanish Pyrenees. Hydrological Sciences
621 Journal, 49(5): 787-802. https://doi.org/10.1623/hysj.49.5.787.55135

622 López-Moreno JI, Gascoin S, Herrero J, Sproles EA, Pons M, Alonso-González
623 E, Hanich L, Boudhar A, Musselman KN, Molotch NP, Sickman J, Pomeroy J. 2017.
624 Different sensitivities of snowpacks to warming in Mediterranean climate mountain
625 areas. Environmental Research Letters, 12(7): L074006. https://doi.org/10.1088/1748-
626 9326/aa70cb.

627 López-Moreno JI, Vicente-Serrano SM. 2007. Atmospheric circulation influence
628 on the interannual variability of snow pack in the Spanish Pyrenees during the second
629 half of the 20th century. Nordic Hydrology, 38(1): 33-44.
630 https://doi.org/10.2166/nh.2007.030.

631 Mankin JS, Diffenbaugh NS. 2015. Influence of temperature and precipitation
632 variability on near-term snow trends. Climate Dynamics, 45(3): 1099–1116.
633 https://doi.org/10.1007/s00382-014-2357-4.

634 Mann HB. 1945. Nonparametric Tests Against Trend. Econometrica, 13(3):
635 245–259. https://doi.org/10.2307/1907187.

636 Marchane A, Jarlan L, Hanich L, Boudhar A, Gascoin S, Tavernier A, Filali N,
637 Le Page M, Hagolle O, Berjamy B. 2015. Assessment of daily MODIS snow cover
638 products to monitor snow cover dynamics over the Moroccan Atlas mountain range.
639 Remote Sensing of Environment, 160: 72–86.
640 https://doi.org/https://doi.org/10.1016/j.rse.2015.01.002.

641 Marke T, Hanzer F, Olefs M, Strasser U. 2018. Simulation of Past Changes in
642 the Austrian Snow Cover 1948-2009, J. Hydrometeor., 19: 1519-1545.
643 https://doi.org/10.1175/JHM-D-17-0245.1

644 Martin E, Etchevers P. 2005. Impact of Climatic Changes on Snow Cover and
645 Snow Hydrology in the French Alps. In: Huber U.M., Bugmann H.K.M., Reasoner
646 M.A. (eds) Global Change and Mountain Regions. Advances in Global Change
647 Research, vol 23. Springer, Dordrecht.

648 Marty C. 2008. Regime shift of snow days in Switzerland. Geophysical
649 Research Letters. John Wiley & Sons, Ltd, 35(12).
650 https://doi.org/10.1029/2008GL033998.

651 Marty C, Tilg A-M, Jonas T. 2017. Recent Evidence of Large-Scale Receding
652 Snow Water Equivalents in the European Alps. Journal of Hydrometeorology.
653 American Meteorological Society, 18(4): 1021–1031. https://doi.org/10.1175/JHM-D-
654 16-0188.1.

655 Morán-Tejeda E, López-Moreno JI, Sanmiguel-Vallelado A. 2017. Changes in
656 Climate, Snow and Water Resources in the Spanish Pyrenees: Observations and
657 Projections in a Warming Climate BT - High Mountain Conservation in a Changing
658 World. In: Catalan J, Ninot JM and Aniz MM (eds) Springer International Publishing:
659 Cham, 305–323.

660 Morán-Tejeda E, Moreno J, Beniston M. 2013. The changing role of
661 temperature, precipitation and elevation on snowpack variability in Switzerland.
662 Geophys. Res. Lett., 40: 2131– 2136, doi:10.1002/grl.50463.

663 Morin S, Horton S, Techel F, Bavay M, Coléou C, Fierz C, Gobiet A,
664 Hagenmuller P, Lafaysse M, Ližar M, Mitterer C, Monti F, Müller K, Olef M, Snook
665 JS, van Herwijnen A, Vionnet V. Application of physical snowpack models in support
666 of operational avalanche hazard forecasting : a status report on current implementations
667 and prospects for the future. Cold. Reg. Sci. Technol., 170: 102910,
668 https://doi.org/10.1016/j.coldregions.2019.102910, 2020.

669 Mote, P.W., Li, S., Lettenmaier, D.P., Xiao, M., Engel, R. 2018. Dramatic
670 declines in snowpack in the western US. npj Clim Atmos Sci 1, 2. doi:10.1038/s41612-
671 018-0012-1

672 Musselman KN, Clark MP, Liu C, Ikeda K, Rasmussen R. 2017. Slower
673 snowmelt in a warmer world. Nature Climate Change, 7(3): 214–219.
674 https://doi.org/10.1038/nclimate3225.

675 Navarro-Serrano F, López-Moreno JI. 2017. Spatio-temporal analysis of
676 snowfall events in the Spanish pyrenees and their relationship to atmospheric
677 circulation. Cuadernos de Investigacion Geografica, 43(1): 233-254.
678 https://doi.org/10.18172/cig.3042.

679 Pérez-Zanón N, Sigró J, Ashcroft L. 2017. Temperature and precipitation
680 regional climate series over the central Pyrenees during 1910–2013. International
681 Journal of Climatology, 37(4): 1922–1937. https://doi.org/10.1002/joc.4823.

682 Pierce D, Cayan D. 2013. The Uneven Response of Different Snow Measures to
683 Human-Induced Climate Warming. Journal of Climate, 26: 4148–4167.
684 https://doi.org/10.1175/JCLI-D-12-00534.1.

685 Pons M, Johnson P, Rosas-Casals M, Sureda B, Jover E. 2012. Modeling climate
686 change effects on winter ski tourism in Andorra. Climate Research 54(3): 197–207.
687 https://doi.org/10.3354/cr01117.

688 Pons M, López-Moreno JI, Rosas-Casals M, Jover È. 2015. The vulnerability of
689 Pyrenean ski resorts to climate-induced changes in the snowpack. Climatic Change,
690 131(4): 591-605. https://doi.org/10.1007/s10584-015-1400-8.

691 Rasouli K, Pomeroy JW, Janowicz JR, Carey SK, Williams TJ. 2014.
692 Hydrological sensitivity of a northern mountain basin to climate change. Hydrological
693 Processes, 28(14): 4191–4208. https://doi.org/10.1002/hyp.10244.

694 Rasouli K, Pomeroy JW, Whitfield PH. 2019. Are the effects of vegetation and
695 soil changes as important as climate change impacts on hydrological processes? Hydrol.
696 Earth Syst. Sci. Discuss., 2019: 1–33. https://doi.org/10.5194/hess-2019-214.

697 Rohrer M, Salzmann N, Stoffel M, Kulkarni A V. 2013. Missing (in-situ) snow
698 cover data hampers climate change and runoff studies in the Greater Himalayas. Science

699 of The Total Environment, 468–469: S60–S70.
700 https://doi.org/https://doi.org/10.1016/j.scitotenv.2013.09.056.

701 Sanmiguel-Vallelado A, Camarero J, Gazol A, Morán-Tejeda E, Sangüesa-
702 Barreda G, Alonso-González E, Gutiérrez E, Alla A, Galván J, López-Moreno J. 2019.
703 Detecting snow-related signals in radial growth of Pinus uncinata mountain forests.
704 Dendrochronologia, 125622. https://doi.org/10.1016/j.dendro.2019.125622.

705 Schöner W, Koch R, Matulla C, Marty C, Tilg A-M. 2019. Spatiotemporal
706 patterns of snow depth within the Swiss-Austrian Alps for the past half century (1961 to
707 2012) and linkages to climate change. International Journal of Climatology, 39(3):
708 1589–1603. https://doi.org/10.1002/joc.5902.

709 Serrano-Notivoli R, Brustenga A, Prohom M, Cuadrat J, Cunillera J, Trapero L,
710 Pons M, Tejedor E, Saz M, López-Moreno J, copons llorens R, Gascoin S, Luna MY,
711 Rodriguez-Camino E, Ramos-Calzado P, Amblar-Francés P, Soubeyroux J-M. 2019.
712 Observed climatic trends in the Pyrenees (1950-2015). EGU General Assembly 2019,
713 Viena (Austria), DOI:10.13140/RG.2.2.17306.29125

714 Serrano-Notivoli R, Martín-Vide J, Saz MA, Longares LA, Beguería S,
715 Sarricolea P, Meseguer-Ruiz O, de Luis, M. 2018. Spatio-temporal variability of daily
716 precipitation concentration in Spain based on a high-resolution gridded data set. Int. J.
717 Climatol, 38: e518-e530. doi:10.1002/joc.5387

718 Serrano E, de Sanjosé-Blasco JJ, Gómez-Lende M, López-Moreno JI, Pisabarro
719 A, Martínez-Fernández A. 2019. Periglacial environments and frozen ground in the
720 central Pyrenean high mountain area: Ground thermal regime and distribution of
721 landforms and processes. Permafrost and Periglacial Processes, 1-18.
722 https://doi.org/10.1002/ppp.2032.

723 Spandre P, François H, Verfaillie D, Pons M, Vernay M, Lafaysse M, George E,
724 Morin S. 2019. Winter tourism under climate change in the Pyrenees and the French
725 Alps: relevance of snowmaking as a technical adaptation. The Cryosphere, 13(4): 1325–
726 1347. https://doi.org/10.5194/tc-13-1325-2019.

727 Sproles AE, Crumley LR, Nolin WA, Mar E, Lopez-Moreno JI. 2018.
728 SnowCloudHydro—A New Framework for Forecasting Streamflow in Snowy, Data-
729 Scarce Regions. Remote Sensing, 10(8): 1276.

730 Sterl A. 2004. On the (in)homogeneity of reanalysis products, J. Clim., 17(19),
731 3866–3873, doi:10.1175/15200442.

732 Surfleet CG, Tullos D. 2013. Variability in effect of climate change on rain-on-
733 snow peak flow events in a temperate climate. Journal of Hydrology, 479: 24–34.
734 https://doi.org/10.1016/j.jhydrol.2012.11.021.

735 Trigo RM, DaCamara CC. 2000. Circulation weather types and their influence
736 on the precipitation regime in Portugal. International Journal of Climatology. 20(13):
737 1559–1581. https://doi.org/10.1002/1097-0088.

738 van Pelt WJJ, Kohler J, Liston GE, Hagen JO, Luks B, Reijmer CH, Pohjola
739 VA. 2016. Multidecadal climate and seasonal snow conditions in Svalbard. Journal of
740 Geophysical Research: Earth Surface, 121(11): 2100–2117.
741 https://doi.org/10.1002/2016JF003999.

742 Vernay M, Lafaysse M, Hagenmuller P, Nheili R, Verfaillie D, Morin S. 2019.
743 The S2M meteorological and snow cover reanalysis in the French mountainous areas
744 (1958 - present) [Data set]. AERIS. https://doi.org/10.25326/37

745 Verfaillie D, Lafaysse M, Déqué M, Eckert N, Lejeune Y, Morin S. 2018. Multi-
746 components ensembles of future meteorological and natural snow conditions in the
747 Northern French Alps, The Cryosphere, 12: 1249-1271. https://doi.org/10.5194/tc-12-
748 1249-2018, 2018.

749 Vidal JP, Martin E, Franchisteguy L, Baillon M, Soubeyroux JM. 2010. A 50-
750 year high-resolution atmospheric reanalysis over France with the Safran system. Int. J.
751 Climatol., 30(11): 1627–1644, doi:10.1002/joc.2003.

752 Wang X, Wang T, Guo H, Liu D, Zhao Y, Zhang T, Liu Q, Piao S. 2018.
753 Disentangling the mechanisms behind winter snow impact on vegetation activity in

754 northern ecosystems. Global Change Biology, 24(4): 1651–1662.
755 https://doi.org/10.1111/gcb.13930.

756 Wegmann M, Orsolini Y, Dutra E, Bulygina O, Sterin A, Brönnimann S. 2017.
757 Eurasian snow depth in long-term climate reanalyses. The Cryosphere, 11(2): 923–935.
758 https://doi.org/10.5194/tc-11-923-2017.

759 Yue S, Wang CY. 2002. Applicability of prewhitening to eliminate the influence
760 of serial correlation on the Mann-Kendall test. Water Resources Research, 38(6): 4–7.
761 https://doi.org/10.1029/2001WR000861.

762

**Appendix T1.** Average snow duration and snow depth (DJFMA) for each analyzed massif, their corresponding group and Tau-Kendall values for the period 1958-2017. Bold numbers indicate statistically significant trends.

| Massif | Average values | | | | Kendall-Tau and classified group | | | | | | | |
|---|---|---|---|---|---|---|---|---|---|---|---|---|
| | Dur. 1500 | Dur. 2100 | Depth 1500 | Depth 2100 | Dur. 1500 | PC | Dur. 2100 | PC | Depth 1500 | PC | Depth 2100 | PC |
| Pays Basque | 106 | 150 | 0.31 | 1.70 | **-0.42** | 1 | -0.10 | 1 | **-0.38** | 1 | **-0.33** | 1 |
| Aspe-Ossau | 134 | 150 | 0.37 | 1.71 | **-0.27** | 1 | **-0.17** | 1 | **-0.22** | 1 | **-0.23** | 1 |
| Hte. Bigorre | 122 | 148 | 0.18 | 0.93 | -0.15 | 1 | **-0.18** | 1 | -0.10 | 1 | **-0.20** | 1 |
| Aure-Louron | 112 | 148 | 0.19 | 0.93 | **-0.21** | 1 | -0.15 | 1 | **-0.19** | 1 | **-0.28** | 1 |
| Luchonnais | 116 | 148 | 0.23 | 1.03 | **-0.22** | 1 | **-0.17** | 1 | **-0.18** | 1 | **-0.26** | 1 |
| Couserans | 126 | 148 | 0.25 | 1.11 | **-0.19** | 1 | **-0.17** | 3 | -0.08 | 1 | -0.11 | 3 |
| Aran | 99 | 146 | 0.17 | 0.84 | -0.09 | 1 | -0.16 | 3 | 0.07 | 2 | **-0.17** | 1 |
| Hte. Ariege | 122 | 146 | 0.20 | 0.91 | -0.15 | 2 | **-0.21** | 2 | -0.14 | 2 | **-0.18** | 3 |
| Andorre | 66 | 126 | 0.04 | 0.31 | 0.01 | 1 | **-0.23** | 3 | 0.06 | 1 | **-0.25** | 3 |
| Orlu-StBarthe | 118 | 146 | 0.19 | 0.94 | -0.10 | 2 | **-0.23** | 2 | -0.09 | 2 | **-0.21** | 2 |
| Capcir-Puymorens | 67 | 127 | 0.06 | 0.36 | -0.02 | 2 | **-0.18** | 2 | 0.00 | 3 | **-0.18** | 2 |
| Cerdagne | 85 | 120 | 0.05 | 0.40 | **-0.18** | 2 | -0.13 | 4 | **0.17** | 3 | -0.01 | 2 |
| Navarra | 108 | 149 | 0.31 | 1.72 | **-0.31** | 1 | **-0.21** | 1 | **-0.18** | 1 | **-0.19** | 3 |
| Jacetanía | 109 | 149 | 0.22 | 1.44 | **-0.17** | 1 | -0.13 | 4 | -0.11 | 1 | **-0.20** | 3 |
| Gállego | 120 | 148 | 0.24 | 1.40 | -0.10 | 1 | -0.08 | 4 | 0.00 | 1 | -0.15 | 3 |
| Sobrarbe | 127 | 147 | 0.18 | 1.09 | -0.06 | 1 | -0.02 | 4 | 0.06 | 1 | 0.03 | 3 |
| Ésera | 96 | 147 | 0.17 | 0.94 | -0.11 | 1 | **-0.18** | 3 | -0.03 | 1 | -0.14 | 3 |
| Ribagorza | 85 | 146 | 0.16 | 0.89 | -0.11 | 2 | -0.14 | 3 | 0.01 | 2 | **-0.17** | 2 |
| Pallaresa | 100 | 139 | 0.09 | 0.50 | -0.13 | 2 | -0.11 | 2 | **0.17** | 2 | -0.02 | 2 |
| Perafita | 60 | 125 | 0.05 | 0.35 | -0.01 | 2 | **-0.31** | 2 | 0.02 | 3 | **-0.25** | 2 |
| Teruel-Frese | 48 | 123 | 0.06 | 0.40 | **0.18** | 2 | -0.06 | 2 | **0.17** | 2 | 0.09 | 2 |
| Cadi-Moixero | 52 | 126 | 0.05 | 0.39 | **0.17** | 2 | **-0.22** | 2 | 0.11 | 3 | -0.11 | 2 |
| Prepirene | 75 | 130 | 0.07 | 0.48 | 0.08 | 2 | **-0.21** | 4 | 0.04 | 3 | -0.10 | 3 |

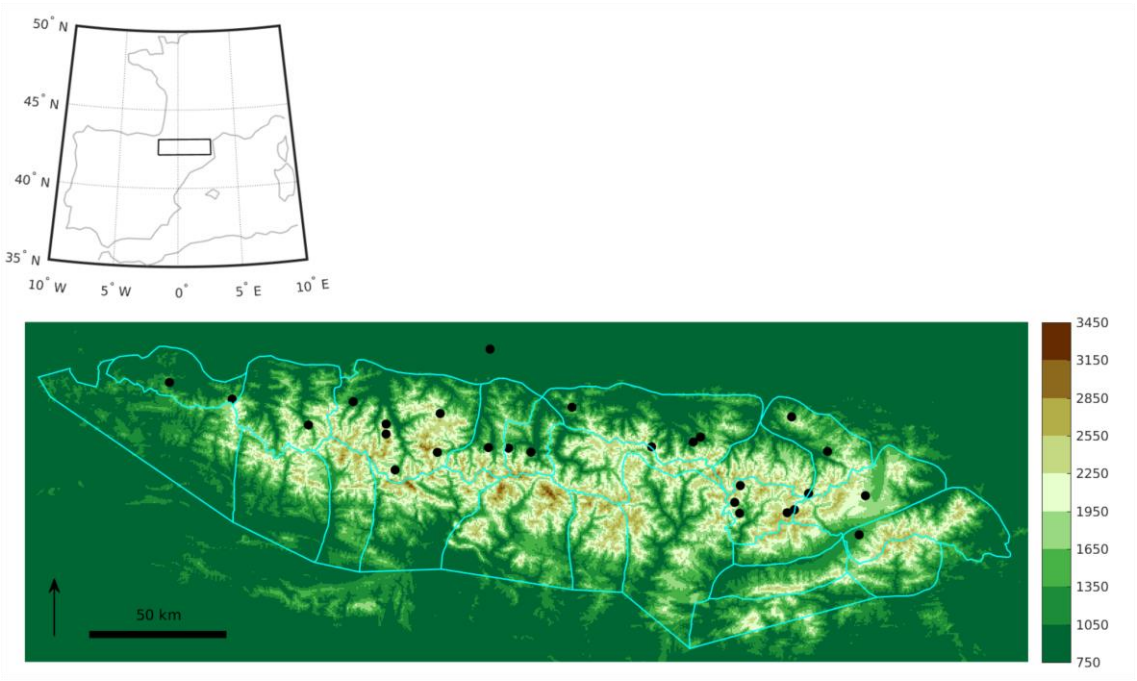


**Figure 1.** The study area, and delimitation of the 23 massifs into which the Pyrenees was divided for the SAFRAN-Crocus simulation. Black dots indicate the location of the snow depth observation stations (full list given in the Appendix T1).

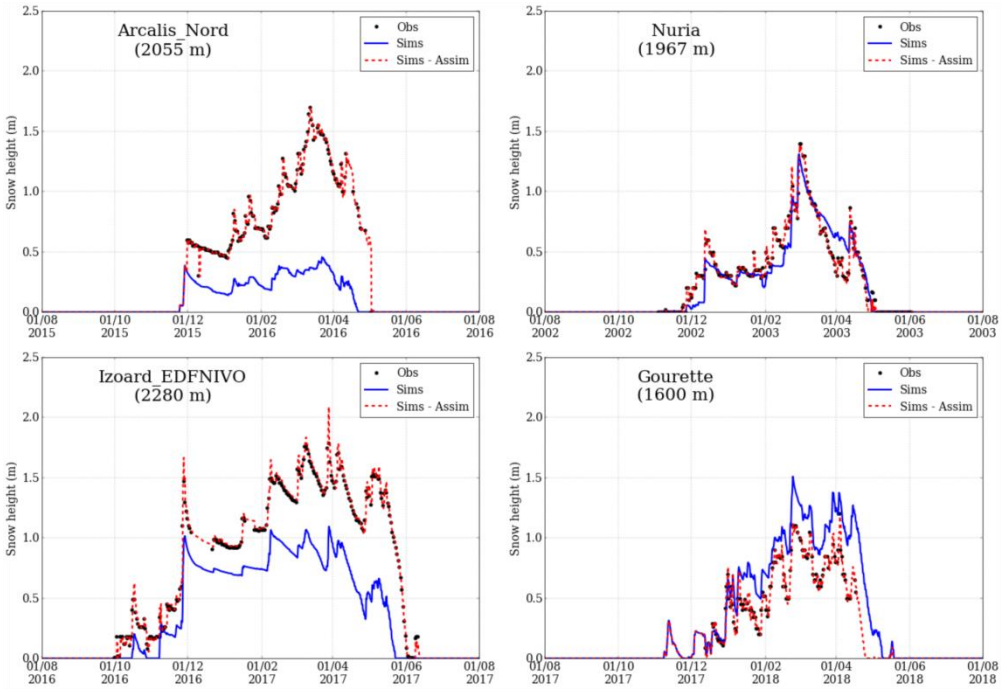


772

773 **Figure 2.** Examples of observed and simulated snow series with SAFRAN Crocus
774 approach in four observatories before (Sims) and after applying the correction
775 procedure explained in this section (Sims- Assim).

776

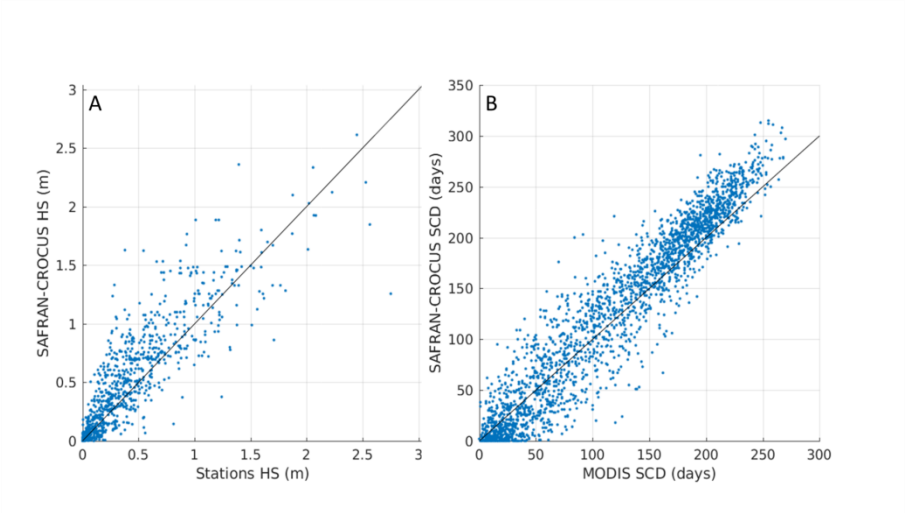


777

778 **Figure 3.** A: Comparison of the mean annual snow depth, as simulated by SAFRAN-
779 Crocus and from the reconstructed station dataset. B: Comparison of the mean annual
780 snow cover duration, as simulated by SAFRAN-Crocus and from the MODIS dataset.
781 Each dot corresponds to a triplet (massif, elevation band, hydrological year).

782

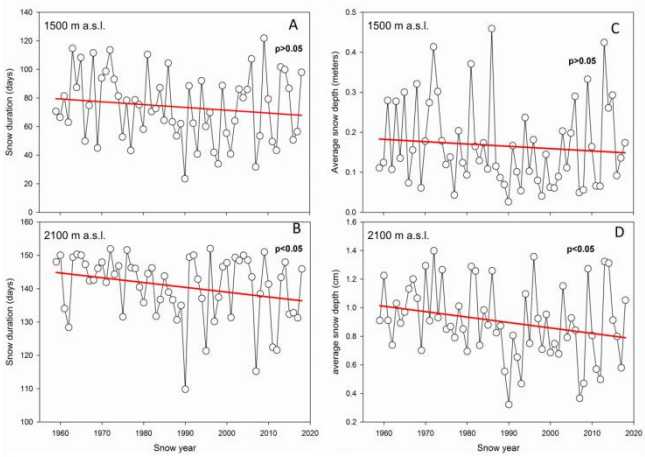


783

784 **Figure 4.** Evolution of annual snow cover duration (A and B) and average snow depth
785 from December to April (C and D) at 1500 and 2100 m a.s.l. respectively.

786

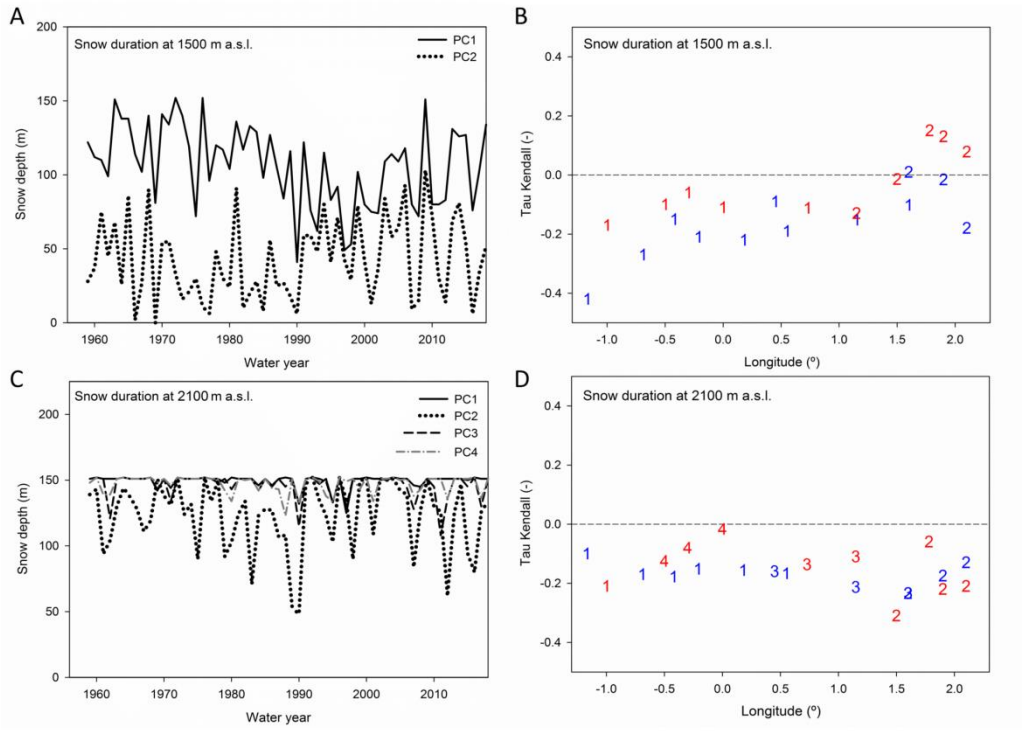


787

788 **Figure 5.** Temporal evolution of the factorial scores for the groups of massifs identified
789 by PCA for the annual evolution of snow cover duration at 1500 m a.s.l. (A) and 2100
790 m a.s.l. (C). Kendall's tau coefficients for the massifs classified in the various groups
791 (numbers) from west to east at 1500 m a.s.l. (B) and 2100 m a.s.l. (D). Those massifs
792 located north of the main divide are shown in blue, and those to the south are shown in
793 red.

794

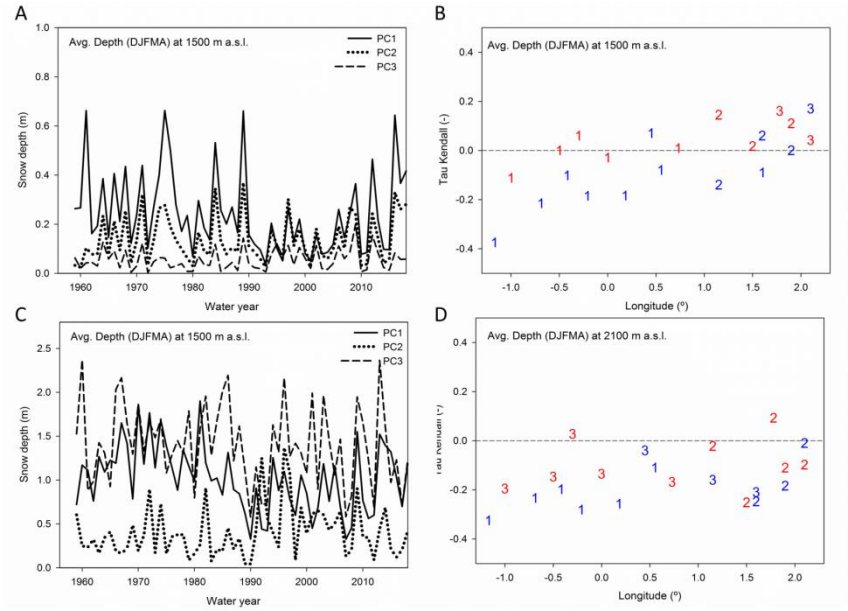


795

796 **Figure 6.** Factorial scores for the groups of massifs identified by principal component
797 analysis for the evolution of snow depth (DJFM) at 1500 m a.s.l. (A) and 2100 m a.s.l.
798 (C). Kendall's tau coefficients for the massifs classified in the various groups (numbers)
799 from west to east at 1500 m a.s.l. (B) and 2100 m a.s.l. (D). Those massifs located north
800 of the main divide are shown in blue, and those to the south are shown in red.

801

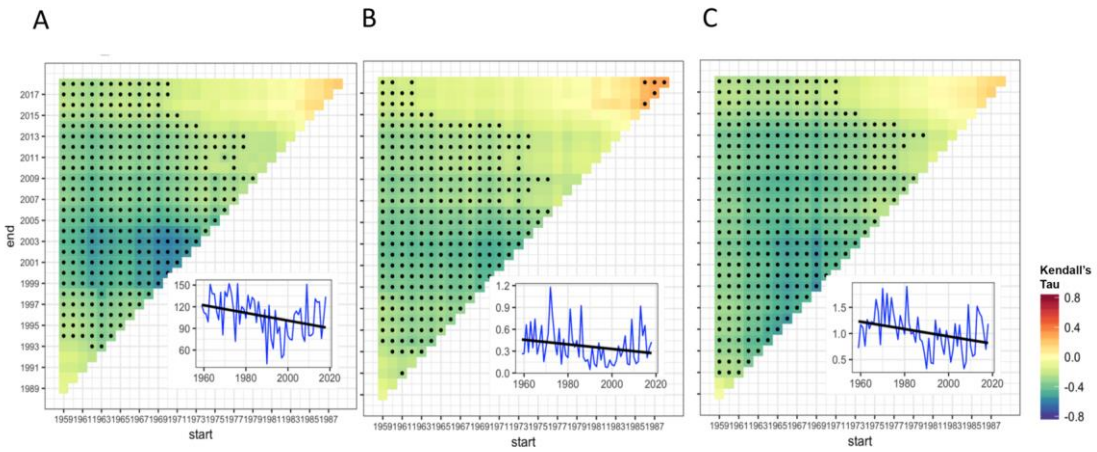


802

803 **Figure 7.** Results of the Mann-Kendall test applied to the observatories that exhibited
804 the largest correlation with those principal components characterized by the strongest
805 negative trends. The matrix shows all possible combinations of start and ending dates
806 involving at least 20 years duration during the period 1958–2017. A) Aspe-Ossau
807 massif for PC1 for snow cover duration at 1500 m a.s.l. B) Navarra massif for PC1 for
808 average snow depth (DJFMA) at 1500 m a.s.l. C) Luchonnais massif for PC1 for
809 average snow depth (DJFMA) at 2100 m a.s.l. Colors indicate the magnitude of the
810 Kendall's tau, and points mark the series that showed statistically significant trends ($p < 0.05$).

812

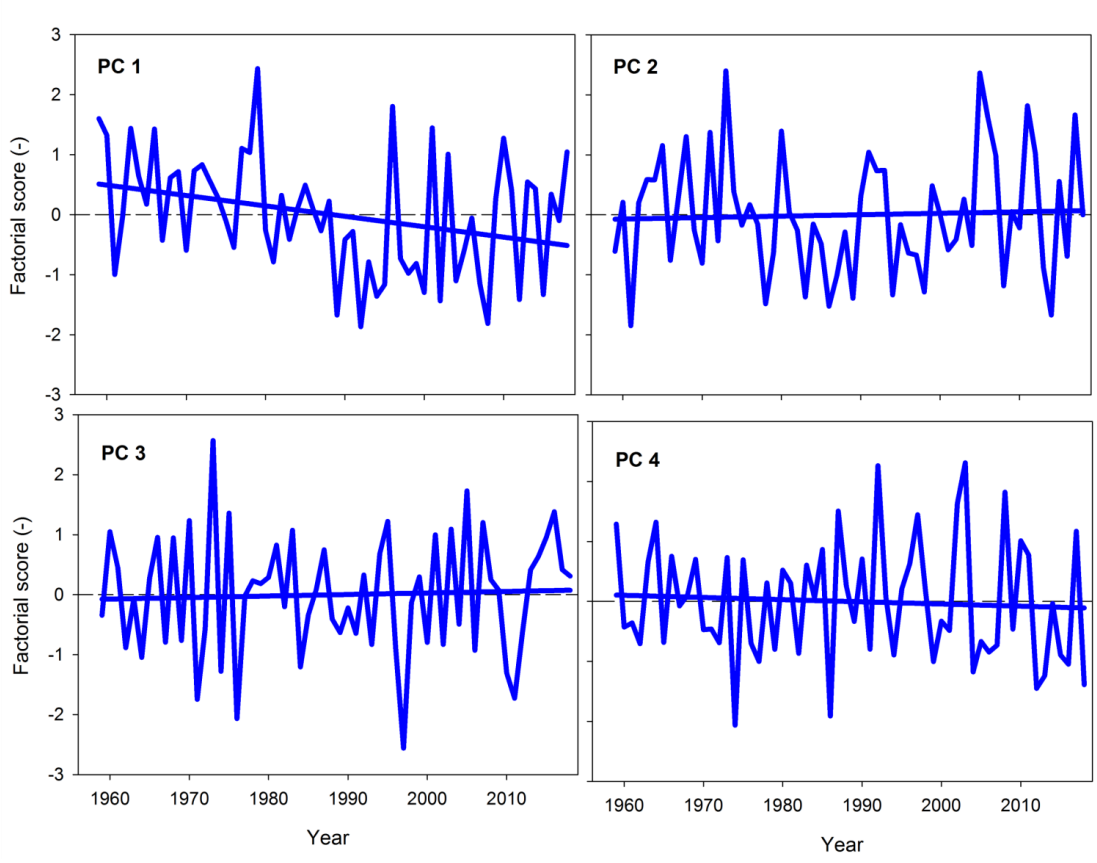


813

814 **Figure 8.** Temporal evolution of the factorial scores for the four principal components
815 that summarized the frequency of weather types over the Pyrenees during the study
816 period.